This article has been accepted for publication in a future issue of this journal, but has not been fully edited. Content may change prior to final publication. Citation information: DOI 10.1109/TAP.2019.2922547, IEEE Transactions on Antennas and Propagation

Communication

Multiband MIMO Microwave and Millimeter Antenna System Employing Dual-function Tapered Slot Structure

Muhammad Ikram, Nghia Nguyen-Trong, *Member, IEEE*, and Amin Abbosh, *Senior Member, IEEE*

***Abstract*—A single-layered multiple-input multiple-output (MIMO) antenna system is presented for future wireless devices operating at WLAN (2.45, 5.2 GHz), 4G LTE (2.6 GHz) and 5G (24, 28 GHz) bands. The design consists of a dual-band 4-element monopole MIMO antenna system that covers 2.45 and 5.2 GHz bands. A decoupling mechanism is designed in the ground plane based on a tapered slot. This tapered slot has a dual function, working both as a decoupling structure ($\lambda_0/4$ long) at 2.45 GHz and as a tapered slot antenna ($3\lambda_0$ long) at 28 GHz when excited by a proper feeder. The proposed MIMO antenna system is designed on an RO-5880 substrate with overall dimensions of $104 \times 104 \times 0.51$ mm^3. The measured results show that the presented design covers two low frequency bands (2.40-2.80, 5.1-5.6 GHz) with peak gain of 5 dBi and one high frequency band (23-30 GHz) with peak gain of 11 dBi. The minimum measured isolation between the two antennas is more than 16 dB, while the maximum envelope correlation coefficient value is less than 0.16 showing good MIMO characteristics.**

***Index Terms*—Multiple-input multiple-output (MIMO), mm-Waves, monopole antenna, tapered slot antenna, WLAN, 4G LTE, 5G.**

I. Introduction

INTEGRATED antenna systems having small antenna footprint and supporting multiple wireless standards (microwave/mm-wave) are highly desirable for small form factor wireless devices. In addition, multiple-input multiple-output (MIMO) antenna technology is one of the most important parts of the future wireless communication system because it increases data throughput without increasing input power and bandwidth [1]–[3]. In fact, the integration of MIMO antenna system in the small form factor wireless devices is challenging due to the high mutual coupling between neighboring antenna elements especially when they are spaced less than $\lambda_0/2$ apart and sharing the same system ground plane [4], [5]. Recently, multi-band antenna designs were reported at microwave and mm-wave bands [6]–[8] for WLAN, WiGig and ISM band applications. In [6], a substrate-integrated antenna was presented at 5.2 and 24 GHz band, while in [7], [8] two geometries were also reported at 2.45, 5.2 and 60 GHz bands. However, the limiting factors in these designs were, either the use of multi-layered structures without having MIMO configuration or a low gain at mm-wave band. A more recent design was presented in [9] for 5G wireless devices that supports only 24 GHz band with moderate gain.

Manuscript received Feb., 2019

M. Ikram, N. Nguyen-Trong and A. Abbosh are with the School of Information Technology and Electrical Engineering, University of Queensland (UQ), Brisbane, 4072 Australia. Corresponding author: M. Ikram. Email: *m.ikram@uq.edu.au*

This work was supported by the Australian Research Council under ARC Grant LP160100917

Some antenna designs were also reported with [10]–[14] and without [15]–[20] MIMO configuration to cover different microwave bands for WLAN, WiFi and LTE applications. Nevertheless, most of the MIMO designs either have multi-layered 3D configuration [10], [13], relatively large size [12], low isolation between MIMO elements [11] or operate in a single band [14], which limit their application for future low-profile, compact and multi-band applications. Furthermore, the designs that cover both microwave and mm-wave bands typically have relatively low gain values at mm-wave bands [6]–[8]. It is also noted that the MIMO designs reported in [10]–[14] only cover microwave bands. The comparison of several notable reported works is shown in Table I. Indeed, none of the presented works cover microwave and mm-wave bands with MIMO configurations.

To solve the aforementioned challenges, this work proposes a MIMO antenna system for microwave and mm-wave band applications. The proposed antenna covers 2.45, 2.6, 5.2, 24 and 28 GHz bands. The design starts with a dual-band monopole MIMO antenna system optimized for 2.45, 2.6 and 5.2 GHz bands. Then, a decoupling structure based on the tapered slot is etched in the ground plane. This tapered slot has a dual function, working both as a decoupling structure at 2.45 GHz and as a tapered slot antenna (or Vivaldi antenna) at 28 GHz. This dual feature of the tapered slot makes the proposed design compact, low profile, and multi-band. MIMO characteristics such as isolation and envelope correlation coefficient are also calculated. Results show that the proposed design meets those MIMO requirements. As shown in Table I, the proposed design has a similar size of reported works in [10]–[14] at microwave frequencies, however, it introduces an additional feature of the tapered slot to cover the mm-wave band with high gain, which is a key requirement for 5G applications.

II. Design Evolution

In this section, the design procedure of dual-band monopole MIMO antenna system, working at 2.45 and 5.2 GHz, is firstly demonstrated. Then, a decoupling feature is designed in the ground plane based on a tapered slot. This tapered slot also works as a high-gain traveling-wave antenna at 28 GHz. Finally, an integrated MIMO antenna system is optimized to cover different bands for WLAN, 4G LTE, and 5G applications. The proposed MIMO antenna system is designed using Rogers RT/duroid 5880 having a relative permittivity of 2.2, a loss tangent of 0.0009 at 10 GHz and the thickness (t) of 0.51 mm.

This article has been accepted for publication in a future issue of this journal, but has not been fully edited. Content may change prior to final publication. Citation information: DOI 10.1109/TAP.2019.2922547, IEEE Transactions on Antennas and Propagation

TABLE I
COMPARISON OF PROPOSED AND PREVIOUS WORKS BASED ON DIFFERENT CRITICAL PARAMETERS.

Ref.	MIMO	Support mm-wave	Size of board (mm^3)	Freq. (GHz) with wireless standards	Realized Gain (dBi) at mm-wave	No. of ports	Isolation (dB) between feeding ports
[10]	Yes	No	$30 \times 30 \times 12.9$ (one element)	WLAN=5.2	-	6	45
[11]	Yes	No	$64 \times 64 \times 1.52$	WLAN=2.45, 5.2 LTE=2.3-3.8	-	8	9
[12]	Yes	No	$140 \times 120 \times 1.6$	WLAN=2.45 LTE=2.6	-	4	15
[13]	Yes	No	$102 \times 102 \times 0.5$ (1 element, 4-ports)	WLAN=2.5, 5 WiMax=3.5	-	16	20
[14]	Yes	No	$120 \times 120 \times 0.76$	WLAN=5.8	-	3	28
[6]	No	Yes	$40 \times 25 \times 1.524$	WLAN=5.2 ISM=24	7	1-low freq. 1-high freq.	35
[7]	No	Yes	$35 \times 33.5 \times 0.254$	WLAN=2.45, 5.2, 5.8 WiGig=60	6	1-low freq. 1-high freq.	20
[8]	No	Yes	$15 \times 15 \times 0.48$	WLAN=2.4, 5.2, 60	15	1-low freq. 1-high freq.	-
[9]	Yes	Yes	$31.2 \times 31.2 \times 1.57$	5G=24	6.4	8-high freq.	15
This Work	**Yes**	**Yes**	**$104 \times 104 \times 0.51$**	**WLAN=2.45, 5.2 LTE=2.6 5G=24, 28**	**11**	**4-low freq. 4-high freq.**	**16**

A. Design of Dual-band Monopole Antenna with MIMO Configuration

Fig. 1(a) shows the geometry of a dual-band monopole antenna. It is designed on the top layer, while the ground plane is on the bottom layer of an edge-cut square-shaped substrate. The proposed monopole antenna (Ant. 1) consists of two main radiating arms with lengths of L_1 and L_2. It is fed from a 50 Ω transmission line connected to a 50 Ω SMA connector (Fig. 1(a)). The size of the feeding line is $L_f = 22.5$ mm and $w_f = 1.57$ mm, respectively. The lengths L_1 and L_2 are optimized to cover multiple WLAN and LTE bands at 2.45, 2.6 and 5.2 GHz (Fig. 1(b)).

After the optimization of the monopole design (Ant. 1), a copy (Ant. 2) is placed perpendicularly to the Ant. 1 as shown in Fig. 1(c). S-parameters of this 2-element MIMO antenna system are shown in Fig. 1(d). Both antennas cover 2.05-2.71 and 5.06-5.45 GHz bands. As expected, strong mutual coupling is observed between Ant. 1 and Ant. 2. This can be verified from the simulated current distributions (when Ant. 1 is excited and Ant. 2 is terminated with matched load) shown in Fig. 2(c). The minimum isolation is observed as 8 dB between Ant. 1 and Ant. 2, while it varies from 8 to 13 dB in the whole covered lower band.

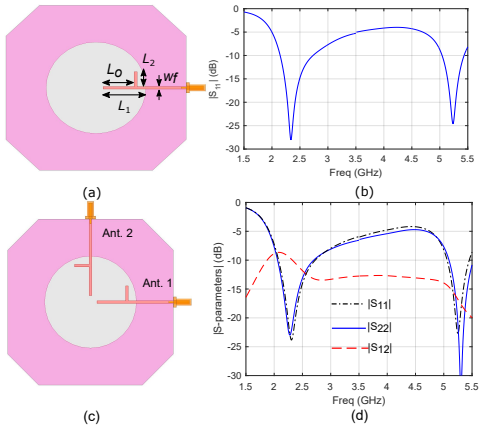

Fig. 1. (a) Dual-band monopole antenna and (b) its simulated reflection coefficient, (c) MIMO antenna system and (d) its simulated performance.

B. Design of Decoupling Tapered Slot

A decoupling mechanism is now designed to improve the isolation between the MIMO antenna elements described in section II.A. Firstly, a narrow rectangular slot is placed in the middle of MIMO antennas in the ground plane (Fig. 2(a)). The length of the slot is $L_{\text{slot}} = 26$ mm which is about $0.2\lambda_0$ at 2.45 GHz. Fig. 3(a) demonstrates the effects of adding this slot, i.e. the resonance is shifted to the higher frequency and the impedance matching becomes slightly worse. Nevertheless, both antenna elements still cover the targeted bands at 2.45 and 2.6 GHz. It can be observed that the slot significantly enhances the isolation between the two antennas. This is due the fact that the slot, which is excited through the coupling from the monopole, becomes a resonator and acts as a band stop filter. This technique is called defected ground structure (DGS) and demonstrated in [21], [22].

The rectangular slot is now replaced by a tapered slot (Figs. 2(b) and 2(d)). It has a similar behavior as a rectangular slot [23], nevertheless, more degrees of freedom for performance optimization is provided. Interestingly, the tapered slot can work as a Vivaldi antenna (details are given in Section II.C) for wideband high gain 5G applications. The closed side of the tapered slot ends with a circular stub that has a diameter of d_{slot}, while the open side has a width of W_{slot}.

This article has been accepted for publication in a future issue of this journal, but has not been fully edited. Content may change prior to final publication. Citation information: DOI 10.1109/TAP.2019.2922547, IEEE Transactions on Antennas and Propagation

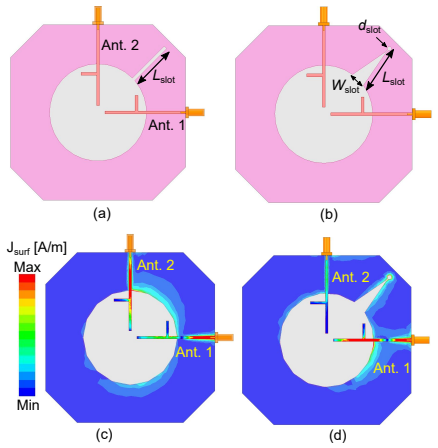

Fig. 2. Monopole MIMO antenna system with (a) rectangular slot and (b) tapered slot and simulated current distributions (c) without tapered slot and (d) with tapered slot.

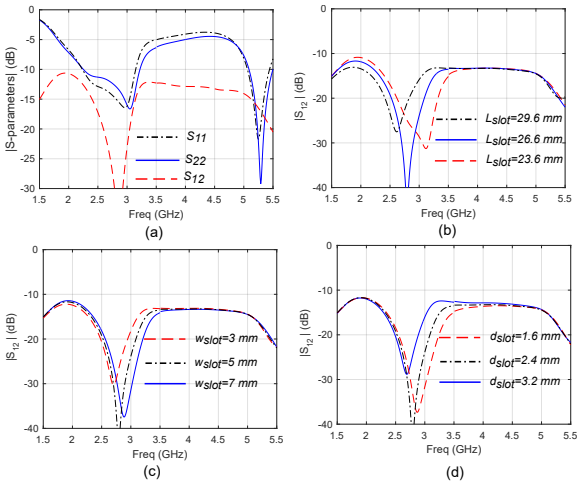

Fig. 3. (a) S-parameters of monopole MIMO antenna with rectangular slot. (b) $|S_{12}|$ of monopole MIMO antenna with tapered slot for L_{slot}, (c) W_{slot} and (d) d_{slot}.

The diameter (d_{slot}) of the circular stub, width (W_{slot}) and length (L_{slot}) of the tapered slot are critical parameters for isolation. Moreover, since this tapered slot will be used for 5G application, those values should be chosen according to the design of end-fire, wideband tapered slot antenna demonstrated in [24] (see next section). A parametric study is performed based on three critical parameters L_{slot}, W_{slot} and d_{slot} of the tapered slot as shown in Figs. 3(b), (c) and (d), respectively. Results show that, as the value of d_{slot} and W_{slot} increase the bandwidth of the isolation also increases, while the value of L_{slot} can be used to shift the band of isolation. Finally, it is noted that adding the slot does not have significant effect on the radiation pattern of the monopole, which is not shown here for brevity.

C. Tapered Slot Antenna

A tapered 50-Ω microstrip line is designed to excite the tapered slot as a Vivaldi antenna to cover 5G band at 28 GHz (Fig. 4). Due to the large frequency gap, the operation of the slot at 28 GHz is independent from the bandstop filter at 2.45 GHz. This dual function of the tapered slot makes the design compact and suitable for multi-standards future wireless devices. The microstrip line is terminated with $\lambda_o/4$ circular stub, which in conjunction with the tapered slot can be used to improve the impedance matching and bandwidth [25], [26]. The location of L_x and L_y of the feeder are optimized to get satisfactory results.

TABLE II
EFFECTS OF L_{SLOT} AND W_{SLOT} ON ISOLATION OF MONOPOLE MIMO ANTENNA AND GAIN OF 5G ANTENNA

W_{slot} (mm)	L_{slot} (mm)	Bandwidth (-10 dB)	Isolation (dB) in covered band	Gain (dBi) at 28 GHz
3	29.6	2.34-3.11	min=15 max=29	10.25
5	29.6	2.32-3.10	min=17 max=28	11.14
7	29.6	2.27-3.25	min=14 max=37	11.52
5	23.6	2.24-3.30	min=13 max=32	9.66
5	26.6	2.35-3.20	min=15 max=40	10.24

The tapered slot works as a Vivaldi antenna [24] and its gain depends on the slot width W_{slot} and length L_{slot}. The S-parameters and radiation patterns at 28 GHz are shown in Figs. 4. The effect of W_{slot} and L_{slot} of the tapered slot on the performance of 5G band is also confirmed by full-wave simulation. It is found that gain of the 5G antenna depends on the width and length of the slot: the gain increases if either the width or length of the slot is increased. However, these parameters also affect the performance of the monopole antenna as studied in Fig. 3. Therefore, a compromise is needed to select the final values. Table II summarizes the performances for different combinations of W_{slot} and L_{slot}. The best case for gain is observed when $W_{\text{slot}} = 7$ mm and $L_{\text{slot}} = 29.6$ mm. The gain increases by increasing the value of W_{slot}, however, this provides worse impedance matching with minimum isolation of 14 dB at lower frequency band. As a compromise between the performance at low and high operating bands, the final optimized parameters are chosen as $W_{\text{slot}} = 5$ mm and $L_{\text{slot}} = 29.6$ mm, providing a gain of 11.14 dB at 28 GHz with minimum isolation of 17 dB across all lower frequency covered bands. The improvement in the isolation can also be verified from the simulated current distributions (when Ant. 1 is excited and Ant. 2 is terminated with matched load) shown in Fig. 2(d) where a low mutual coupling is observed between Ant. 1 and Ant. 2 compared to Fig. 2(c).

III. Results and Discussions

A complete geometry of the MIMO antenna system is shown in Fig. 5(a). All antenna elements are symmetrically arranged in a square shaped substrate. The total size of the board is $104 \times 104 \times 0.51$ mm^3. Due to 4 monopole antenna elements placed next to each other for 4G, WLAN bands and the change in the ground plane structure after adding 4 tapered slots for 5G band, a slight change in the performance

This article has been accepted for publication in a future issue of this journal, but has not been fully edited. Content may change prior to final publication. Citation information: DOI 10.1109/TAP.2019.2922547, IEEE Transactions on Antennas and Propagation

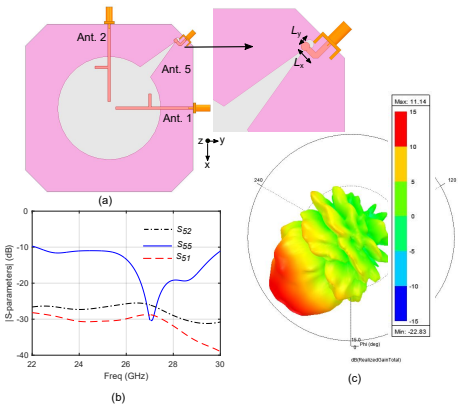

Fig. 4. (a) Geometry of monopole MIMO antenna with tapered slot antenna, (b) simulated S-parameters, and (c) 3D realized gain pattern at 28 GHz.

TABLE III
OPTIMIZED DESIGN PARAMETERS WITH THEIR VALUES

Parameter	Value (mm)	Parameter	Value (mm)
W_{sub}	104	L_o	19
L_{sub}	104	L_1	26
t	0.51	L_2	9
W_{slot}	5	w_f	1.57
L_{slot}	29.6	L_x	4.65
d_{slot}	2.4	L_y	3.65

at low frequency is observed. Therefore, the whole structure shown in Fig. 5(a) is slightly re-tuned to obtain desired results. The integrated MIMO antenna system is optimized through a parametric study performed using Ansys High Frequency Structure Simulator (HFSS). All the optimized parameters with their values are given in Table III. To validate the simulation results, an antenna prototype is fabricated (Fig. 5). The measurement results are demonstrated in the following sub-sections.

A. Scattering Parameters and Comparison

The reflection coefficients for Ant. 1 to Ant. 4 are shown in the Fig. 6(a) for low frequency bands with good agreement between simulations and measurement. It is confirmed that Ant. 1 to Ant. 4 support 2.45, 2.6 and 5.2 GHz (WLAN and LTE) bands with -10-dB impedance bandwidth from 2.40 to 2.80 and 5.1 to 5.6 GHz. The isolation among Ant.1 to Ant. 4 is more than 16 dB (Fig. 6(b)), showing at least 8 dB improvement (compared to Fig. 1(d)). It is noticed from Table IV that the proposed design has a comparable isolation improvement with the other existing decoupling mechanisms such as Electromagnetic Band-Gap (EBG) structure [27], and Neutralization line [28]. The low temperature co-fired ceramic (LTCC) based chip [29] can provide high isolation improvement but with much higher complexity. With lower design complexity, the proposed design provides an additional feature to work at 5G band which is not possible in [27]–[29].

The reflection coefficients for Ant. 5 to Ant. 8 are shown in the Fig. 6(c), while isolation curves are shown in Fig. 6(d) for high frequency band. Results show that Ant. 5 to Ant. 8

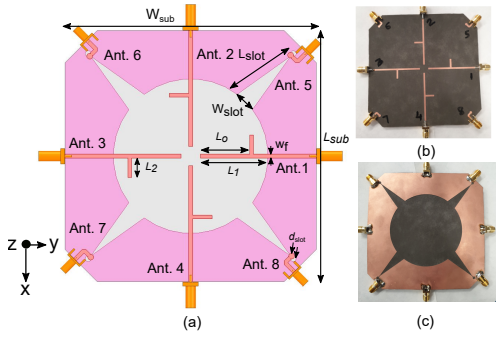

Fig. 5. (a) Geometry of the proposed MIMO antenna system and photograph of the fabricated prototype (b) top view, and (c) bottom view.

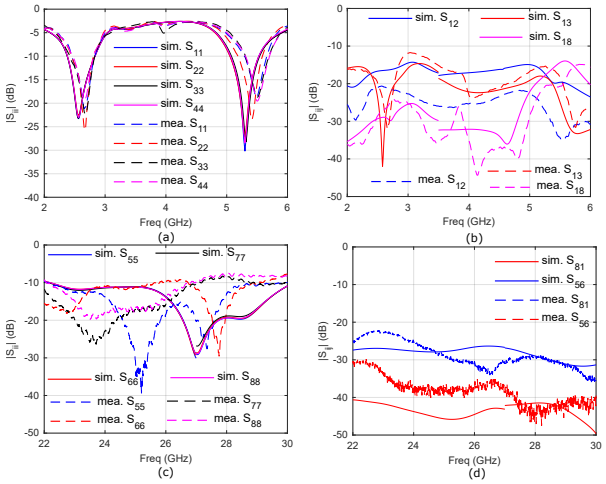

Fig. 6. S-parameters for proposed MIMO antenna system (a) reflection coefficient at low frequency band, (b) isolation at low frequency band, (c) reflection coefficient at high frequency band, and (d) isolation at high frequency band.

have wide bandwidths from 23 to 30 GHz, which support the 24 and 28 GHz bands for 5G applications [30]. The slight difference at high frequencies in the simulations and measurements is mostly due to the fabrication tolerance and soldering of connectors, which is expected for mm-wave designs. The measured isolation is more than 20 dB between low and high frequency ports.

B. Radiation Patterns, ECC, Gain and efficiency

The normalized 2D radiation patterns in terms of total field at $\phi = 0^\circ$ and $\phi = 90^\circ$ for Ant. 1 to Ant. 4 are shown in

TABLE IV
COMPARISON WITH OTHER EXISTING DECOUPLING MECHANISMS

Ref. No.	Minimum improved isolation	Decoupling mechanism	Design complexity
[27]	8 dB	EBG	High
[28]	10 dB	Neutralized line	Moderate
[29]	15 dB	LTCC	High
Proposed	8 dB	Tapered slot	Low

This article has been accepted for publication in a future issue of this journal, but has not been fully edited. Content may change prior to final publication. Citation information: DOI 10.1109/TAP.2019.2922547, IEEE Transactions on Antennas and Propagation

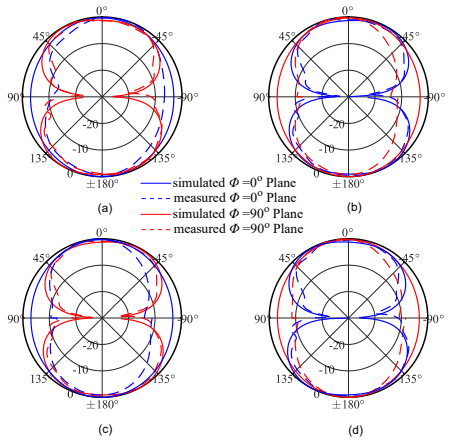

Fig. 7. Normalized radiation patterns at 2.45 GHz, (a) Ant. 1 at $\phi = 0°$ and at $\phi = 90°$, (b) Ant. 2 at $\phi = 0°$ and at $\phi = 90°$, (c) Ant. 3 at $\phi = 0°$ and at $\phi = 90°$, and (d) Ant. 4 at $\phi = 0°$ and at $\phi = 90°$.

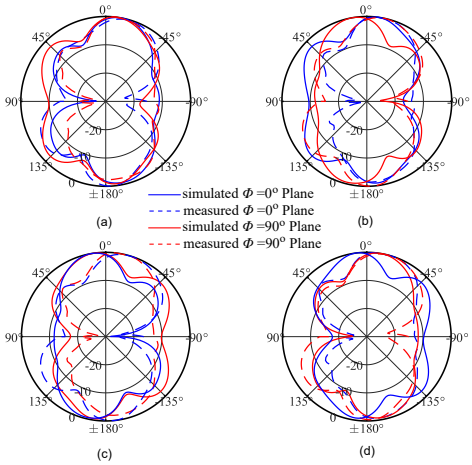

Fig. 8. Normalized radiation patterns at 5.2 GHz, (a) Ant. 1 at $\phi = 0°$ and at $\phi = 90°$, (b) Ant. 2 at $\phi = 0°$ and at $\phi = 90°$, (c) Ant. 3 at $\phi = 0°$ and at $\phi = 90°$, and (d) Ant. 4 at $\phi = 0°$ and at $\phi = 90°$.

Fig. 7 and Fig. 8 at 2.45 and 5.2 GHz, respectively. Omni-directional patterns are obtained for Ant. 1 to Ant.4, which is desired at low frequencies. The discrepancies in the simulated and measured results are attributed to measurement errors, including the cables and measurement setup.

The normalized 2D radiation patterns for Ant. 5 to Ant. 8 are shown in Fig. 9 and Fig. 10 at 24 and 28 GHz. To show the direction of main beam for each antenna, 2D ϕ-cuts at $\theta = 90°$

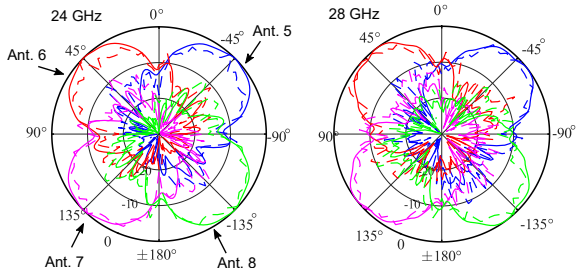

Fig. 9. Normalized radiation patterns at $\theta = 90°$ for 24 GHz and 28 GHz frequencies, measured data: dashed lines; simulated data: solid lines.

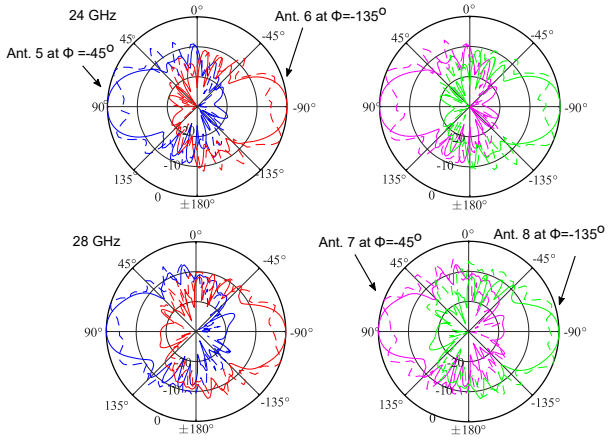

Fig. 10. Normalized radiation patterns at 24 GHz and 28 GHz for different values of ϕ, measured data: dashed lines; simulated data: solid lines.

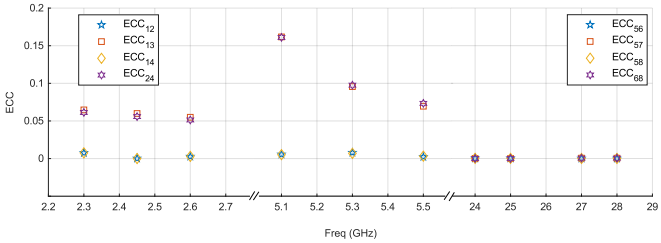

Fig. 11. Calculated ECC values at WLAN and LTE bands (Ant. 1-Ant. 4) and 5G band (Ant. 5-Ant. 8).

are shown in Fig. 9, while θ-cuts at $\phi = -45°$for Ant. 5 and Ant. 7, and at $\phi = -135°$ for Ant. 6 and Ant. 8 are shown in Fig. 10. It is clear that Ant. 5 to Ant. 8 have directional patterns which are desirable at high frequency. Moreover it leads to a very low correlated communication channels. Some gain drop is seen in the measured results at $\pm 90°$ (Fig. 10), which is attributed to the effect of the antenna bending in measurement due the thin and flexible substrate.

The envelope correlation coefficient (ECC) showing the diversity performance of MIMO antenna system is computed using the method given in [4] based on 3D radiation patterns. Fig. 11 shows different values of ECC between different antennas (two antennas at a time) at low frequency bands

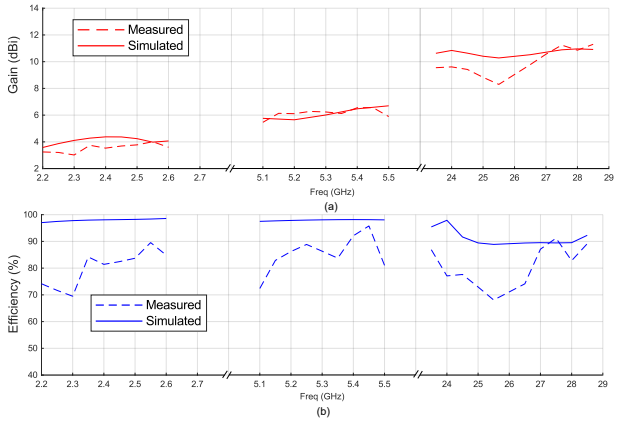

Fig. 12. Simulated and measured (a) peak realized gain and (b) radiation efficiency at WLAN, LTE and 5G bands.

and high frequency band. Due to the same polarization, the maximum ECC value of 0.16 is observed between Ant. 1 and Ant. 3 at 5.1 GHz. Nevertheless, it is still less than the accepted value of 0.5. All other values (see Fig. 11) are also less than the defined value that shows good MIMO diversity performance. ECC values at 5G band are very low (around 0.0001) due to highly directive beams. Another figure of merit at mm-wave band is the beam coverage efficiency (η_c) which is calculated using the procedure in [31]. It is found that the η_c is more than 18%. A higher value of η_c can be achieved with larger number of antennas at mm-wave band. For example, numerical simulation indicates a more than 33% of η_c with 8 antennas while still keeping the same isolation improvement of 8 dB.

The simulated and measured gain and efficiency at WLAN, LTE and 5G bands are shown in Fig.12 (a) and Fig.12 (b), respectively. The maximum measured gain is 4 dBi and 11 dBi at 2.6 GHz and 27.6 GHz, respectively with good agreement between simulation and measurement. The lower measured efficiency is attributed to the higher losses in antenna materials and the measurement errors. Nevertheless, a measured efficiency of more than 70% (average of about 80%) is obtained across all bandwidths.

IV. Conclusion

A multiple-input multiple-output (MIMO) antenna system has been presented for future wireless devices. The proposed design consists of 4-element dual-band monopole and 4-element wideband tapered slot MIMO antenna system that covers different bands for WLAN (2.45, 5.2 GHz), 4G LTE (2.6 GHz) and 5G (24, 28 GHz) applications. The key feature is to design and optimize the tapered-ground slot for dual functions, both as a decoupling structure at 2.45 GHz and as an end-fire tapered slot antenna at 28 GHz. The peak gain of 11 dBi is achieved at 28 GHz with the radiation efficiency of more than 85%. The measured isolation is more than 16 dB in all covered bands. The dual function of the tapered slot makes this dual-band design compact and low profile. The proposed concept can be tailored and applied in different situations, including future access points, wireless routers, and WiFi applications.

References

[1] W. Hong, "Solving the 5G Mobile Antenna Puzzle: Assessing Future Directions for the 5G Mobile Antenna Paradigm Shift," *IEEE Microw. Mag.*, vol. 18, no. 7, pp. 86–102, Nov 2017.

[2] J. G. Andrews, S. Buzzi, W. Choi, S. V. Hanly, A. Lozano, A. C. K. Soong, and J. C. Zhang, "What Will 5G Be?" *IEEE J. Sel. Areas Commun.*, vol. 32, no. 6, pp. 1065–1082, June 2014.

[3] M. Ikram, Y. Wang, M. S. Sharawi, and A. Abbosh, "Dual band circular mimo antenna system for 5g wireless devices," in *2018 IEEE Int. Symp. on Antennas and Propag. USNC/URSI National Radio Science Meeting*, July 2018, pp. 247–248.

[4] M. S. Sharawi, "Printed Multi-Band MIMO Antenna Systems and Their Performance Metrics [Wireless Corner]," *IEEE Antennas Propag. Mag.*, vol. 55, no. 5, pp. 218–232, Oct 2013.

[5] M. A. Jensen and J. W. Wallace, "A review of antennas and propagation for MIMO wireless communications," *IEEE Trans. Antennas Propag.*, vol. 52, no. 11, pp. 2810–2824, Nov 2004.

[6] Y. Sun and K. W. Leung, "Substrate-Integrated Two-Port Dual-Frequency Antenna," *IEEE Trans. Antennas Propag.*, vol. 64, no. 8, pp. 3692–3697, Aug 2016.

[7] D. Wang and C. H. Chan, "Multiband Antenna for WiFi and WiGig Communications," *IEEE Antennas Wireless Propag. Lett.*, vol. 15, pp. 309–312, 2016.

[8] T. Zhihong, Y. P. Zhang, C. Luxey, A. Bisognin, D. Titz, and F. Ferrero, "A Ceramic Antenna for Tri-Band Radio Devices," *IEEE Trans. Antennas Propag.*, vol. 61, no. 11, pp. 5776–5780, Nov 2013.

[9] N. Shoaib, S. Shoaib, R. Y. Khattak, I. Shoaib, X. Chen, and A. Perwaiz, "Mimo antennas for smart 5g devices," *IEEE Access*, vol. 6, pp. 77 014–77 021, 2018.

[10] W. Han, X. Zhou, J. Ouyang, Y. Li, R. Long, and F. Yang, "A Six-Port MIMO Antenna System With High Isolation for 5-GHz WLAN Access Points," *IEEE Antennas Wireless Propag. Lett.*, vol. 13, pp. 880–883, 2014.

[11] M. Ikram, M. S. Sharawi, and A. Shamim, "Compact circular connected monopole antenna arrays for wideband MIMO applications," *IET Microw., Antennas Propag.*, vol. 12, no. 13, pp. 2122–2127, 2018.

[12] A. MoradiKordalivand, T. A. Rahman, and M. Khalily, "Common Elements Wideband MIMO Antenna System for WiFi/LTE Access-Point Applications," *IEEE Antennas Wireless Propag. Lett.*, vol. 13, pp. 1601–1604, 2014.

[13] Y. Pan, Y. Cui, and R. Li, "Investigation of a Triple-Band Multibeam MIMO Antenna for Wireless Access Points," *IEEE Trans. Antennas Propag.*, vol. 64, no. 4, pp. 1234–1241, April 2016.

[14] S. S. Jehangir and M. S. Sharawi, "A Wideband Sectoral Quasi-Yagi MIMO Antenna System with Multi-Beam Elements," *IEEE Trans. Antennas Propag.*, pp. 1–1, 2018.

[15] Y. Liu, H. Kim, and H. Kim, "Loop-Type Ground Radiation Antenna for Dual-Band WLAN Applications," *IEEE Trans. Antennas Propag.*, vol. 61, no. 9, pp. 4819–4823, Sep. 2013.

[16] T. V. Hoang and H. C. Park, "Very simple 2.45/3.5/5.8 GHz triple-band circularly polarised printed monopole antenna with bandwidth enhancement," *Electronics Letters*, vol. 50, no. 24, pp. 1792–1793, 2014.

[17] C. Lin, C. Huang, and G. Chen, "Obtuse Pie-Shaped Quasi-Self-Complementary Antenna for WLAN Applications," *IEEE Antennas Wireless Propag. Lett.*, vol. 12, pp. 353–355, 2013.

[18] M. Z. M. Nor, S. K. A. Rahim, M. I. Sabran, P. J. Soh, and G. A. E. Vandenbosch, "Dual-Band, Switched-Beam, Reconfigurable Antenna for WLAN Applications," *IEEE Antennas Wireless Propag. Lett.*, vol. 12, pp. 1500–1503, 2013.

[19] H. Huang, Y. Liu, and S. Gong, "Broadband Dual-Polarized Omnidirectional Antenna for 2G/3G/LTE/WiFi Applications," *IEEE Antennas Wireless Propag. Lett.*, vol. 15, pp. 576–579, 2016.

[20] S. Maddio, "A Circularly Polarized Switched Beam Antenna With Pattern Diversity for WiFi Applications," *IEEE Antennas Wireless Propag. Lett.*, vol. 16, pp. 125–128, 2017.

[21] C. Luo, J. Hong, and L. Zhong, "Isolation Enhancement of a Very Compact UWB-MIMO Slot Antenna With Two Defected Ground Structures," *IEEE Antennas Wireless Propag. Lett.*, vol. 14, pp. 1766–1769, 2015.

[22] C. Chiu, C. Cheng, R. D. Murch, and C. R. Rowell, "Reduction of mutual coupling between closely-packed antenna elements," *IEEE Trans. Antennas Propag.*, vol. 55, no. 6, pp. 1732–1738, June 2007.

[23] S. Tebache, A. Belouchrani, F. Ghanem, and A. Mansoul, "Novel reliable and practical decoupling mechanism for strongly coupled antenna arrays," *IEEE Trans. Antennas Propag.*, pp. 1–1, 2018.

[24] P. J. Gibson, "The Vivaldi Aerial," in *1979 9th European Microw. Conf.*, Sep. 1979, pp. 101–105.

[25] K. Ebnabbasi, D. Busuioc, R. Birken, and M. Wang, "Taper design of vivaldi and co-planar tapered slot antenna (tsa) by chebyshev transformer," *IEEE Trans. Antennas Propag.*, vol. 60, no. 5, pp. 2252–2259, May 2012.

[26] D. Yang, S. Liu, and D. Geng, "A Miniaturized Ultra-Wideband Vivaldi Antenna With Low Cross Polarization," *IEEE Access*, vol. 5, pp. 23 352–23 357, 2017.

[27] F. Yang and Y. Rahmat-Samii, "Microstrip antennas integrated with electromagnetic band-gap (EBG) structures: a low mutual coupling design for array applications," *IEEE Trans. Antennas Propag.*, vol. 51, no. 10, pp. 2936–2946, Oct 2003.

[28] S. Zhang and G. F. Pedersen, "Mutual Coupling Reduction for UWB MIMO Antennas With a Wideband Neutralization Line," *IEEE Antennas Wireless Propag. Lett.*, vol. 15, pp. 166–169, 2016.

[29] L. Zhao, F. Liu, X. Shen, G. Jing, Y. Cai, and Y. Li, "A High-Pass Antenna Interference Cancellation Chip for Mutual Coupling Reduction of Antennas in Contiguous Frequency Bands," *IEEE Access*, vol. 6, pp. 38 097–38 105, 2018.

[30] Federal Communications Commission (FCC), "The FCC's 5G FAST Plan, Spectrum," https://www.fcc.gov/5G.

[31] J. Helander, K. Zhao, Z. Ying, and D. Sjoberg, "Performance Analysis of Millimeter-Wave Phased Array Antennas in Cellular Handsets," *IEEE Antennas Wireless Propag. Lett.*, vol. 15, pp. 504–507, 2016.